Supporting Information

Influence of one specific carbon–carbon bond on the quality, stability, and photovoltaic performance of hybrid organic–inorganic bismuth–iodide materials

David M. Fabian[†], Alex M. Ganose[‡∣⊥], Joseph W. Ziller[†], David O. Scanlon[‡∣⊥], Matthew C. Beard[⁑], and Shane Ardo[†Δ]*

[†]Department of Chemistry, University of California Irvine, Irvine, CA 92697-2025, United States

[‡]Department of Chemistry, University College London, 20 Gordon Street, London WC1H 0AJ, United Kingdom

[∣]Diamond Light Source, Harwell Campus, Didcot OX11 0DE, United Kingdom

[⊥]Thomas Young Centre, University College London, Gower Street, London WC1E 6BT, United Kingdom

[⁑]National Renewable Energy Laboratory, Golden, Colorado 80401, United States

[Δ]Department of Chemical Engineering and Materials Science, University of California Irvine, Irvine, CA 92697-2025, United States

Additional Experimental

X-ray Data Collection and Structure Solution for (HDA^{2+})BiI$_5$

        A red crystal of approximate dimensions 0.125 x 0.127 x 0.276 mm was mounted on a glass fiber and transferred to a Bruker SMART APEX II diffractometer. The APEX2[S1] program package was used to determine the unit-cell parameters and for data collection (10 sec/frame scan time for a sphere of diffraction data). The raw frame data was processed using SAINT[S2] and SADABS[S3] to yield the reflection data file. Subsequent calculations were carried out using the SHELXTL[S4] program. The diffraction symmetry was *mmm* and the systematic absences were consistent with the orthorhombic space groups *Pnma* and *Pna*2$_1$. It was later determined that space group *Pna*2$_1$ was correct.

        The structure was solved by dual space methods and refined on F^2 by full-matrix least-squares techniques. The analytical scattering factors[S5] for neutral atoms were used throughout the analysis. Hydrogen atoms were included using a riding model. It was necessary to refine carbon atoms isotropically (presumably due to high absorption). The complex formed an extended structure.

        Least-squares analysis yielded wR2 = 0.0646 and Goof = 1.150 for 100 variables refined against 3940 data (0.78 Å), R1 = 0.0282 for those 3844 data with I > 2.0σ(I). The structure was refined as an inversion twin. The predicted powder pattern displayed in Figure 2a was solved using Mercury software.

X-ray Data Collection and Structure Solution for (PA$^+$)$_x$BiI$_y$

        An orange crystal of approximate dimensions 0.062 x 0.109 x 0.216 mm was mounted in a cryoloop and transferred to a Bruker SMART APEX II diffractometer. The APEX2 program package was used to determine the unit-cell parameters and for data collection (15 sec/frame scan time for a sphere of diffraction data). The raw frame data was processed using SAINT and SADABS to yield the reflection data file. Subsequent calculations were carried out using the SHELXTL program. There were no systematic absences nor any diffraction symmetry other than the Friedel condition. The centrosymmetric triclinic space group $P\bar{1}$ was assigned and later determined to be correct.

The structure was solved by direct methods and refined on F^2 by full-matrix least-squares techniques. The analytical scattering factors for neutral atoms were used throughout the analysis. Hydrogen atoms were included using a riding model. Disordered atoms were included using multiple components with partial site-occupancy-factors.

Least-squares analysis yielded wR2 = 0.1406 and Goof = 1.180 for 193 variables refined against 6628 data (0.82 Å), R1 = 0.0685 for those 5553 data with $I > 2.0\sigma(I)$. The predicted powder pattern displayed in Figure 2b was solved using Mercury software.

Structure Solution Definitions

wR2 = $[\Sigma[w(F_o^2-F_c^2)^2] / \Sigma[w(F_o^2)^2]]^{1/2}$

R1 = $\Sigma||F_o|-|F_c|| / \Sigma|F_o|$

Goof = S = $[\Sigma[w(F_o^2-F_c^2)^2] / (n-p)]^{1/2}$ where n is the number of reflections and p is the total number of parameters refined.

The thermal ellipsoid plot is shown at the 50% probability level.

Density Functional Theory Calculations for $(HDA^{2+})BiI_5$

All density functional theory (DFT) calculations were performed using the Vienna *Ab initio* Simulation Package (VASP), employing the projector augmented-wave (PAW) method to describe the interactions and between valence and core electrons. A Γ-centered 2x2x1 *k*-point sampling mesh was found to achieve convergence to within 1 meV/atom. The plane wave energy cutoff was converged to 10 meV/atom, with a cutoff of 400 eV found to be sufficient. To prevent errors arising from Pulay stress, the cutoff energy was raised to 520 eV during geometry relaxations. The structures were deemed converged when the forces on each atom totaled less than 10 meV/Å.

Geometry relaxations were performed using the PBEsol functional, a version of the Perdew Burke and Ernzerhof (PBE) functional revised for solids. PBEsol has been shown to accurately reproduce the structure parameters of many materials containing post-transition metal cations. To avoid errors arising from the systematic band gap underestimation in generalized gradient approximation functionals such as PBEsol, the Heyd--Scuseria--Ernzerhof hybrid functional (HSE06) was employed for density of states, band structure and optics calculations. In addition,

spin–orbit coupling (SOC) was treated explicitly to account for the relativistic effects on the bismuth valence electrons. This combination of HSE06+SOC has previously been shown to reproduce the electronic properties of a large number of solar absorber materials. The optical response was calculated using density functional perturbation theory (DFPT) within the transversal approximation, in which only direct valence to conduction band transitions are considered.

Supplementary Figures

(a)   **(b)**   **(c)**
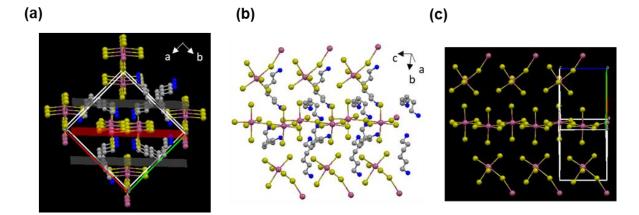

Figure S1. (a) 1 x 1 x 3 unit cell structure of $(HDA^{2+})BiI_5$ with orientation in the [110] direction. The red plane indicates the (110) plane, the gray planes indicate (220) planes, purple spheres = bismuth, gold spheres = iodide, gray spheres = carbon, and blue spheres = nitrogen. (b) The same structure as displayed in panel (a), but rotated 90°. (c) The same structure as displayed in panel (b), but with the hexanediammonium groups removed. For clarity, hydrogens are omitted from all data.

Table S1. Crystallographic data for $(HDA^{2+})BiI_5$.

Empirical formula	$C_6 H_{18} Bi I_5 N_2$
Formula weight	961.70 g/mol
Temperature	128(2) K
Crystal system	Orthorhombic
Space group	$Pna2_1$
a	15.0653(13)
b	14.1204(12)
c	8.6201(8)
α	90 °
β	90 °
γ	90 °
Volume	1833.7(3)
Z	4
Calculated density	3.484 g/cm^3
Absorption coefficient	18.012 mm^{-1}
F(000)	1664
Crystal size	0.276 x 0.127 x 0.125 mm
Crystal color	red
θ range for data collection	1.977 to 27.100°
Index ranges	$-19 \leq h \leq 19$, $-18 \leq k \leq 17$, $-11 \leq l \leq 11$
Reflections collected/unique	18044/3940
Completeness to $\theta = 25.50°$	99.7 %
Absorption correction	Semi-empirical from equivalents

Table S2. Crystallographic data for $(PA^+)_x BiI_y \cdot CH_3OH$.

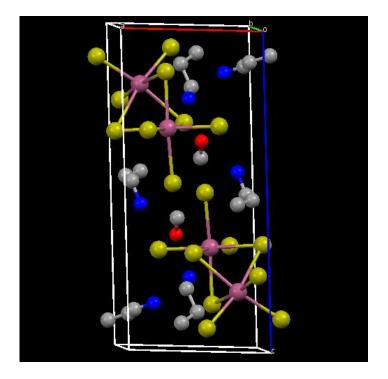|	
Empirical formula	$C_{10} H_{34} Bi_2 I_9 N_3 O$
Formula weight	1772.46
Temperature	88(2) K
Crystal system	Triclinic
Space group	$P\bar{1}$
a	8.4726(10)
b	12.2421(15)
c	17.789(2)
α	92.014(2) °
β	92.398(2) °
γ	108.002(1) °
Volume	1751.0(4)
Z	2
Calculated density	3.362 g/cm³
Absorption coefficient	17.978 mm⁻¹
F(000)	1532
Crystal size	0.216 x 0.109 x 0.062 mm
Crystal color	orange
θ range for data collection	1.147 to 25.679°
Index ranges	$-10 \leq h \leq 10$, $-14 \leq k \leq 14$, $-21 \leq l \leq 21$
Reflections collected/unique	16809/6628
Completeness to $\theta = 25.50°$	99.5 %
Absorption correction	Semi-empirical from equivalents

Figure S2. Unit cell structure of $(PA^+)_x BiI_y \cdot CH_3OH$ from single-crystal growth. Hydrogen atoms are omitted for clarity. Purple spheres = bismuth, gold spheres = iodide, blue spheres = nitrogen, and gray spheres = carbon, and red spheres = oxygen.
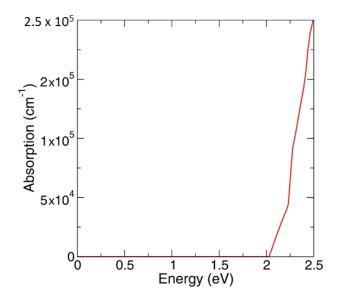

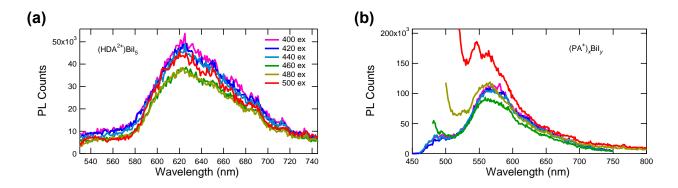**Figure S3**. Calculated optical absorption spectrum of $(HDA^{2+})BiI_5$.

Figure S4. Steady-state photoluminescence spectra at the indicated (ex)citation wavelengths for a thin film of (a) $(HDA^{2+})BiI_5$ and (b) $(PA^+)_xBiI_y$. The key in panel a is also appropriate for panel b.
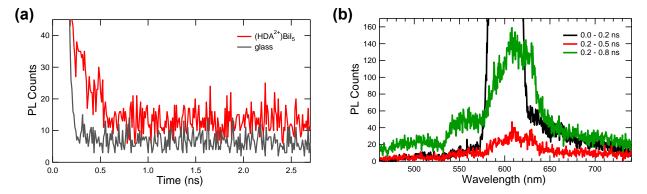

Figure S5. Time-resolved photoluminescence (a) kinetic data and (b) spectra at 410 nm excitation and at the indicated delay times, each from a thin film of $(HDA^{2+})BiI_5$ with 10 wt. % KI incorporated in the precursor solution.
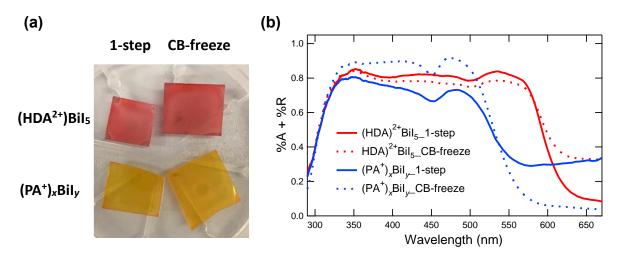
Figure S6. (a) Digital photograph images of the thin films corresponding to each spectrum shown in panel b. (b) Absorptance + reflectance spectra of $(HDA^{2+})BiI_5$ (red) and $(PA^+)_xBiI_y$ (blue) thin films deposited on glass using a conventional one-step deposition (1 step, solid lines) and using a fast deposition crystallization with chlorobenzene as the antisolvent (CB-freeze, dashed lines).
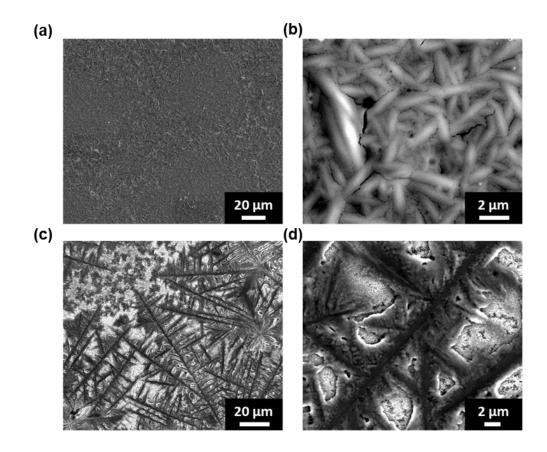
Figure S7. Plan-view scanning electron microscopy images of thin films of (a,b) $(HDA^{2+})BiI_5/mTiO_2/cTiO_2/FTO$ and (c, d) $(PA^+)_xBiI_y/mTiO_2/cTiO_2/FTO$.
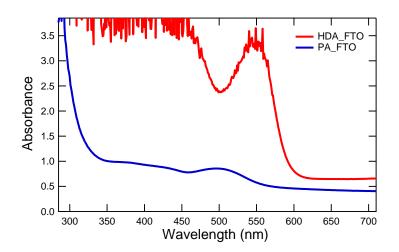

Figure S8. Electronic absorption spectra of thin films of $(HDA^{2+})BiI_5$ and $(PA^+)_xBiI_y$ deposited on fluorine-doped tin–oxide coated glass substrates using the same solution concentrations and spin-coat protocol to produce each film.

References

(S1)   APEX2, 2014.

(S2)   SAINT, 2013.

(S3)   Sheldrick, G. M. SADABS, 2014.

(S4)   Sheldrick, G. M. SHELXTL, 2014.

(S5)   International Tables for X-Ray Crystallography; Vol C.; Kluwer Academic Publishers: Dordrecht, 1992.